Afro-Asian Journal of Scientific Research (AAJSR)
المجلة الأفروآسيوية للبحث العلمي
E-ISSN: 2959-6505
Volume 4, Issue 3, 2026
Page No: 134-142
Website: https://aajsr.com/index.php/aajsr/index
SJIFactor 2024: 5.028 ISI 2025: 0.915 معامل التأثير العربي (AIF) 2025: 0.76

DFT-Based Analysis of Structure-Activity Relationships of Some Tetrazole Compounds as Corrosion Inhibitors on Carbon Steel in HCl.

Mahmud Ibrahim Elusta[1*], Ahmed Khalid Jarnaz[2], Emel Bayol[3]
[1]Materials Science Engineering, Libyan Authority for Scientific Research, Tripoli – Libya
[2]Engineering project management, Libyan Authority for Scientific Research, Tripoli – Libya
[3]Department of Metallurgy and Materials Engineering, Faculty of Engineering, Niğde Ömer Halisdemi University, Niğde, Türkiye

تحليل قائم على نظرية الكثافة الوظيفية لعلاقات التركيب والنشاط لبعض مركبات التترازول كمثبطات للتآكل على الفولاذ الكربوني في حمض الهيدروكلوريك.

محمود ابراهيم الأسطى[1*]، أحمد خالد جرناز[2]، أمل بايول[3]
[1]هندسة علوم مواد، الهيئة الليبية للبحث العلمي، طرابلس، ليبيا
[2]إدارة المشاريع الهندسية، الهيئة الليبية للبحث العلمي، طرابلس، ليبيا
[3]قسم هندسة علوم مواد، كلية الهندسة، جامعة نيدة عمرحالص دمير، نيدة، تركيا.

*Corresponding author: Elustam@aonsrt.ly

Received: May 17, 2026	Accepted: July 25, 2026	Published: August 11, 2026

Abstract:
This study presents a comprehensive quantum chemical analysis of tetrazole (TZ) derivatives as potential inhibitors of iron corrosion in dilute hydrochloric acid (HCl). Investigations were carried out in the presence of. Absence of three compounds: 5-Phenyl Tetrazole, 5-Amino tetrazole and Tetrazole was evaluated in neutral and protonated forms in gas phase and water phase conditions. The thing is, all theoretical calculations were carried out using the density functional theory (DFT) method at the B3LYP/6-311++G(2d,2p) level, which aims to determine the correlation between molecular structure and corrosion inhibitory activity. A complete set of quantum chemical descriptors, including frontier molecular orbital energy, energy gap (ΔE), ionization potential, global hardness, and softness. Electrophilicity index, chemical potential, electronegativity, and Mulliken atomic charge are calculated systematically. Correlation analysis was performed to set up the relationship between these descriptors and the inhibition efficiency of the molecules studied. At the risk of stating the obvious (and this is key), these findings offer valuable molecular-level insights into the adsorption behavior and inhibition mechanisms of tetrazole derivatives on iron surfaces.

Keywords: Corrosion, tetrazole, Efficiency, Analysis, density.

الملخص:
تُقدِّم هذه الدراسة تحليلاً كموميًا شاملاً لمشتقات التترازول (Tetrazole, TZ) بوصفها مثبطات محتملة لتآكل الحديد الكربون في محلول مخفف من حمض الهيدروكلوريك (HCl). وقد شملت الدراسة ثلاثة مركبات، هي: 5-فينيل تترازول (5-Phenyl Tetrazole)، و5-أمينو تترازول(5-Amino Tetrazole) ، والتترازول(Tetrazole) ، حيث جرى

تقييمها في صورتيها المتعادلة والبروتونية، وفي كلٍّ من الطور الغازي والطور المائي. أُجريت جميع الحسابات النظرية باستخدام نظرية دالة الكثافة (Density Functional Theory, DFT) عند مستوى B3LYP/6-311++G(2d,2p)، بهدف تحديد العلاقة بين التركيب الجزيئي وكفاءة تثبيط التآكل. وشملت الدراسة حساب مجموعة متكاملة من الواصفات الكيميائية الكمومية، تضمنت: طاقات المدارات الجزيئية الحدّية (HOMO)،(LUMO) وفجوة الطاقة(ΔE) ، وجهد التأين، والصلادة الكلية، والليونة الكلية، ودليل الإلكتروفيلية، والجهد الكيميائي، والسالبية الكهربية، إضافةً إلى الشحنات الذرية وفق تحليل موليكن.(Mulliken Atomic Charges) كما أُجري تحليل ارتباط (Correlation Analysis)لتحديد العلاقة بين هذه الواصفات الكيميائية الكمومية وكفاءة تثبيط التآكل للمركبات المدروسة. وتوفر النتائج المتحصل عليها فهماً متعمقاً على المستوى الجزيئي لسلوك امتزاز مشتقات التترازول على سطح الحديد، وتوضح الآليات المسؤولة عن فعاليتها في تثبيط التآكل.

الكلمات المفتاحية: التآكل، التترازول، الكفاءة، تحليل، الكثافة، الحديد.

Introduction:

Industrial sectors that cause significant economic losses and threaten structural integrity highlight the importance of effective corrosion mitigation. This is crucial for ensuring the safety and durability of industrial equipment. As it turns out, organic corrosion inhibitors, especially nitrogen-containing heterocyclic compounds, have proven effective in reducing metal degradation [1]. Among these, tetrazole (TZ) and its derivatives, including 5-amino tetrazole and 5-phenyl tetrazole, demonstrate strong adsorption abilities and favorable electronic properties, enabling them to form stable protective layers on metal surfaces. Advances in quantum chemical techniques, particularly Density Functional Theory (DFT), offer deeper insights into the molecular mechanisms of corrosion inhibition and facilitate the rational design of highly efficient inhibitors.

This study is designed to investigate how tetrazole and its derivatives behave in both neutral and protonated forms under gas-phase and aqueous-phase conditions, with the aim of simulating and understanding their interactions with iron in a dilute hydrochloric acid environment. It also seeks to correlate quantum chemical descriptors with inhibition efficiency to elucidate the electronic factors governing adsorption and protection [2]. The research addresses key questions regarding the influence of electronic properties and molecular structure on inhibition performance, the predictive value of quantum chemical descriptors, and the effect of environmental factors on inhibitor behavior [3].

Quantum chemical calculations were performed at the DFT/B3LYP/6-311++G(2d,2p) level using Gaussian 09 (Revision A·02), evaluating descriptors such as hardness, Lowest and Highest Occupied Molecular Orbital Energy (HOMO, LUMO) , electronegativity, energy gap, ionization potential, softness, electrophilicity, chemical potential, and Mulliken charges, and correlating these with inhibition efficiencies to guide the design of next-generation tetrazole-based corrosion inhibitors [4]. This study conducts a quantitative analysis of tetrazole derivatives, including 5-phenyl tetrazole and 5-amino tetrazole, via probe and non-protonated forms in a water and non-water phase. A quantum computational program called Gaussian 09 (Rev· A·02) was used in this analysis [5] to calculate a number of quantum chemical parameters, A range of quantum-chemical parameters was calculated, including the energies of the frontier molecular orbitals, namely Lowest and Highest Occupied Molecular Orbital Energy, the energy separation or gap between these orbitals, ΔE1; the ionization energy, IE1; the chemical hardness, η1; the chemical softness, σ1; the global electrophilicity, ω1; the chemical potential, ε1; and the electronegativity, χ1.

Mulliken atomic charges were also determined for the nitrogen atoms in the both not protonated and non-protonated states. For the aqueous phase, the energy calculations were performed using the 6-311++G(2d,2p) basis set. The connection between the calculated quantum-chemical parameters and the inhibition efficiency was subsequently examined and discussed. Molecular optimization for compounds containing different functional groups, together with the interpretation of the resulting data, has been broadly used and reported in numerous studies [6].

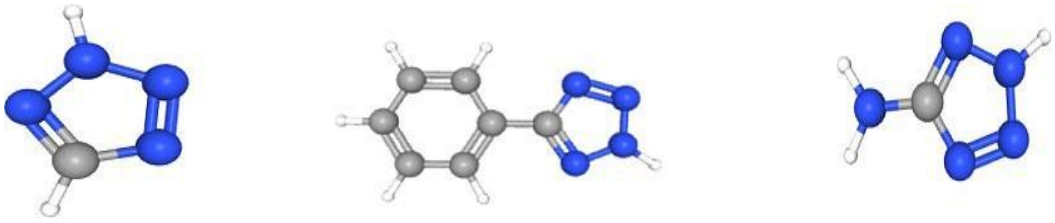

Figure (1): Chemical structures of examined tetrazole and tetrazole derivatives.

Computational Details:

Investigation of the corrosion inhibition mechanisms was carried out through quantum chemistry calculations, as described below. The input files for all molecules examined in this study were generated using GaussView (6.0.16) [4]. Each molecular structure was then subjected to a complete geometry optimization at the B3LYP/6-311++G(2d,2p) level of theory. This basis set is widely recognized for producing reliable molecular geometries and accurate electronic properties for a broad range of organic compounds [9]. In addition, the Gaussian program was used with the basic equation form of the polarized continuum model to represent the influence of water on both neutral and protonated inhibitor molecules. Through this approach, the solvent environment was taken into account when evaluating the molecular geometry and several electronic parameters [10]. A schematic illustration of the compounds investigated in this work is provided in Figure 2, where the number and specific positions of the nitrogen heteroatoms are clearly identified.

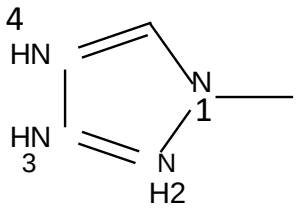

Figure (2): Chemical structures of the investigated tetrazole derivatives

The investigated the chemical parameters of quantum, together with their definitions and the corresponding equations employed for their calculation, are summarized below.

$$A = -E_{LUMO} \quad (1)$$

$$I = -E_{HOMO} \quad (2)$$

$$\mu = -\chi \cong \left(\frac{E_{HOMO} + E_{LUMO}}{2} \right) \quad (3)$$

$$I = -E_{HOMO} \quad (4)$$

$$\chi \cong -\left(\frac{E_{HOMO} + E_{LUMO}}{2} \right) = \frac{I + A}{2} \quad (5)$$

$$\omega = \frac{\chi^2}{2\eta} \quad (6)$$

$$\sigma = \frac{1}{\eta} \cong -\left(\frac{2}{E_{HOMO} - E_{LUMO}} \right) \quad (7)$$

Density Functional Theory (DFT) methods have gained significant traction and usefulness in recent years for investigating corrosion inhibition mechanisms [10]. For this study's quantum chemical calculations, the input files for the molecules under scrutiny were prepared using Gaussian 09 View (6.0.16). A comprehensive optimization was executed with the B3LYP/6-311++G(2d,2p) basis set, renowned for delivering precise geometries and electronic properties across a broad spectrum of organic compounds. The Gaussian program utilized the basic equation form of the polarizable continuous model to simulate the water effect on the geometry and various electronic parameters of both neutral and protonated inhibitor molecules [11]. A schematic representation of the compounds examined can be found in Figure 2, where the number and position of nitrogen heteroatoms are clearly indicated.

Results and Discussion:

Quantum chemical calculations and molecular modeling techniques are extensively employed to assess molecules regarding their reactivity, shape, and binding properties [11]. Parameters like EHOMO, ELUMO, energy gap (ΔE), ionization energy, electron affinity, chemical hardness and softness, dipole moment, proton affinity, electronegativity, electrophilicity, and nucleophilicity offer significant insights for theoretically estimating a molecule's inhibition efficiency. Based on frontier molecular orbital (FMO) theory, a molecule's chemical reactivity is significantly influenced by these factors depends on the interaction between the HOMO and LUMO levels of the reacting species [12-14].

The highest or lowest unoccupied molecular orbitals are referred to as frontier orbitals, and their energies play a fundamental role in determining the molecular reactivity or stability of a compound. E_{HOMO} and E_{LUMO} are widely used parameters associated with, respectively, the electron-donating and electron-accepting ability of molecules [15,16]. The Highest Occupied Molecular Orbital contains electrons of high energy and functions as an electron-donor orbital, whereas the LUMO functions as an electron-acceptor orbital. The corrosion inhibition performance of molecules can be predicted based on the energies of these orbitals. Frontier molecular orbital theory suggests that molecules with a high E_{HOMO} value are effective corrosion inhibitors because they can donate electrons to the metal surface.

On the other hand, E_{LUMO} indicates a molecule's ability to accept electrons, and a molecule with a low E_{LUMO} value can also act as a strong corrosion inhibitor by protecting the metal surface from degradation [17]. The theory is also beneficial in pinpointing the adsorption centers of inhibitor molecules that interact with surface metal atoms. As shown in Figure 3, the charge density distributions for the Lowest and Highest Occupied Molecular Orbital levels of tetrazoles reveal that the HOMO distributions are primarily around the tetrazole ring in all the tetrazole derivatives analyzed in this study. Additionally, in the phenyl tetrazole molecule, these distributions are found around the C=N bond of the phenyl ring and around the amino group in the tetrazole derivative molecule

LUMO orbitals Tetrazole molecules	HOMO orbitals Tetrazole molecules	Optimized geometry	LUMO orbitals Tz -w	HOMO orbitals Tz -w
	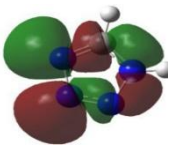	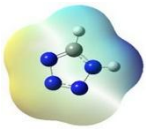 Tetrazole (Tz)	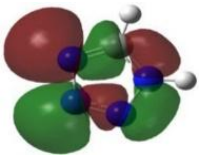	

LUMO orbitals *5-Ph-Tz*	*LUMO* orbitals *5-Ph-Tz*	Optimized geometry ***5-****Phenyl Tetrazole*	LUMO orbitals *5-Ph-Tz -w*	HOMO orbitals *5-Ph-Tz -w*
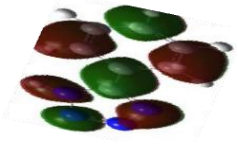		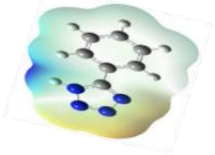		
LUMO o$_{rbitals}$ *5N-H2 -Tz*	**HOMO $_{orbitals}$** *5N-H2 -Tz*	**Optimized geometry** *5-Amino tetrazole (5NH$_2$ -Tz)*	**LUMO orbitals** *5NH2 -Tz -w*	HOMO orbitals *5N-H2 -Tz -w*
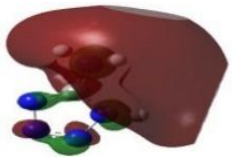	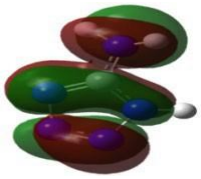	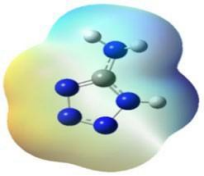	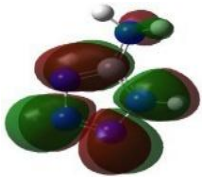	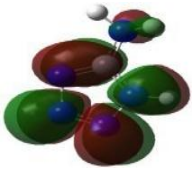

Figure (3): Spatial distributions of the Optimized geometry for the Highest Occupied Molecular Orbital Energy electron densities for the investigated inhibitors in their aqueous-phase (w) and neutral forms, calculated at the B3LYP/6-311++G(2d,2p) level of theory.

Tetrazole (the parent compound) offers multiple nitrogen adsorption sites but has limited electron-donating power. 5-Phenyl-tetrazole adds a donor effect, resulting in strong surface binding. 5-Amino-tetrazole increases π-conjugation and surface π-interactions, though it may introduce steric effects; it also increases electron density via the –NH_2 group and can form hydrogen bonds. Overall, the expected inhibition ranking (qualitative) is: 5-Ph-Tz > 5-NH_2-Tz > Tz.

Table (1): Calculated energy gap (ΔE) and Highest Occupied Molecular Orbital Energy values for the protonated(x) non-protonated(xq) compounds in the gas and aqueous phases at the B3LYP/6-311++G(2d,2p) level of theory.

Compounds (Mwt)	ΔE	ELUMO	EHOMO	Compounds (Mwt)	ΔE	ELUMO	EHOMO
5-Ph-Tz -2x	4.10	-7.22	-11.32	5-Ph-Tz -2xq	5.33	-1.94	-7.27
5-Ph-Tz -3x	4.18	-7.05	-11.23	5-Ph-Tz -3xq	4.77	-2.99	-7.76
5-Ph-Tz -4x	4.88	-6.85	-11.73	5-Ph-Tz -4xq	5.02	-2.98	-8.00
5NH2 -Tz -2x	5.74	-7.16	-12.90	5NH2 -Tz -2 xq	5.66	-2.65	-8.30
5NH2 -Tz -3x	5.43	-7.25	-12.69	5NH2 -Tz -3 xq	5.44	-2.74	-8.18
5NH2 -Tz -4x	7.04	-6.30	-13.34	5NH2 -Tz -4 xq	6.61	-1.99	-8.60
Tz -2x	6.30	-8.27	-14.57	Tz -2 xq	6.80	-3.28	-10.08
Tz -3x	7.42	-8.03	-15.45	Tz -3 xq	7.47	-3.12	-10.59
Tz -4x	7.67	-7.44	-15.11	Tz -4 xq	8.13	-2.42	-10.55

Here's the calculated energy gap valuables were comparison across all nine investigated molecules using the two basis-set variants, protonated(x) and not protonated(xq). The 5-Ph-Tz derivatives exhibited the lowest energy gap values, generally ranging from approximately 4 to 5 eV. In contrast, the unsubstituted Tz derivatives showed the largest energy gaps, with values between 6.3 and 8.1 eV, whereas the 5-NH_2-Tz derivatives displayed intermediate values. The relatively smaller energy gap values obtained for the 5-Ph-Tz derivatives indicate greater electronic responsiveness and a potentially higher tendency to participate in interactions with the metal surface. The ionization energy values (I) is

a fundamental quantum chemical parameter for evaluating molecular reactivity. Higher ionization energy values indicate that the removal of an electron requires greater energy and are generally associated with enhanced electronic stability and lower chemical reactivity.

Conversely, a lower ionization energy suggests that electron removal is more favorable, reflecting a greater tendency of the molecule to participate in electron-donation interactions. Another important quantum chemical descriptor is ionization energy valuable (I). It can be used to assess the electronic reactivity of atoms and molecules [20]. For the protonated species in the gas phase, the calculated ionization energies follow the order 5-Ph-Tz < 5-NH_2-Tz < Tz, with values of 7.36, 11.73, and 12.90 eV, respectively. This trend is consistent with the predicted inhibition performance, which follows the order 5-Ph-Tz > 5-NH_2-Tz > Tz. The particularly low ionization energy of 5-Ph-Tz indicates that its electrons can be removed more readily, suggesting a greater tendency toward electronic interactions with the metal surface and, consequently, a higher inhibition efficiency than those of 5-NH_2-Tz and Tz. As presented in Tables 2 and 3, tetrazole (Tz) exhibits the lowest predicted inhibition efficiency among the investigated compounds in both cases forms, irrespective of whether the calculations are performed in the gas or aqueous phase.

Table (2): Additional calculated results of the quantitative chemistry of the tetrazole derivatives examined at the B3LYP/6-311++G(2d,2p) theoretical level.

Compounds	MV	TNC	Energy	χ,	ω	I	η	σ	ε	μ	Energy
5-Ph-Tz	110.24	-1.74	-13315.42	4.60	3.97	7.27	2.67	0.38	-4.60	6.04	-13315.42
5NH2 -Tz	51.98	-0.85	-8534.94	4.18	2.75	7.35	3.17	0.32	-4.18	6.22	-8534.94
Tz	56.28	-0.39	-7028.34	4.72	3.04	8.38	3.66	0.27	-4.72	5.41	-7028.34

Table (3): Additional calculated quantum chemical descriptors of the not protonated and non-protonated compounds in the aqueous phase and gas phases at the B3LYP/6-311++G(2d,2p) level of theory.

Compounds	**χ**	**TNC**	**ω**	**η**	**ε**	**μ**	**I**	**σ**
Tz -2x	4.11	-0.77	2.60	3.25	-4.11	5.18	7.36	0.31
Tz -3x	4.47	-1.63	3.55	2.81	-4.47	6.89	7.28	0.36
Tz -4x	4.60	-1.74	3.97	2.67	-4.60	6.04	7.27	0.38
Tz -2xq	4.09	-0.88	2.62	3.19	-4.09	6.92	7.27	0.31
Tz -3xq	4.33	-1.69	3.16	2.96	-4.33	9.23	7.29	0.34
Tz -4xq	4.50	-1.92	3.79	2.67	-4.50	8.02	7.18	0.37
5-Ph-Tz -2x	9.27	-1.62	20.94	2.05	-9.27	6.43	11.73	0.49
5-Ph-Tz -3x	9.14	-1.73	19.98	2.09	-9.14	4.26	11.23	0.48
5-Ph-Tz -4x	9.29	-1.34	17.67	2.44	-9.29	1.01	11.32	0.41
5-Ph-Tz -2xq	4.60	-1.92	3.97	2.67	-4.60	9.36	8.00	0.38
5-Ph-Tz -3xq	5.38	-1.83	6.06	2.39	-5.38	6.41	7.76	0.42
5-Ph-Tz -4xq	5.49	-1.40	6.00	2.51	-5.49	0.43	7.27	0.40
5NH2 -Tz -2x	10.03	-0.53	17.54	2.87	-10.03	5.89	12.90	0.35
5NH2 -Tz -3x	9.97	-0.53	18.29	2.72	-9.97	2.16	12.69	0.37
5NH2 -Tz -4x	9.82	-0.27	13.70	3.52	-9.82	6.08	13.34	0.28
5NH2 -Tz -2xq	5.47	-0.63	5.30	2.83	-5.47	7.49	8.30	0.35
5NH2 -Tz -3xq	5.46	-0.61	5.47	2.72	-5.46	2.64	8.18	0.37
5NH2 -Tz -4xq	5.30	-0.32	4.24	3.31	-5.30	7.53	8.60	0.30
Tz -2xq	4.09	-0.88	2.62	3.19	-4.09	6.92	7.27	0.31
Tz -3xq	4.33	-1.69	3.16	2.96	-4.33	9.23	7.29	0.34
Tz -4xq	4.50	-1.92	3.79	2.67	-4.50	8.02	7.18	0.37
5NH2 -Tz -2x	10.03	-0.53	17.54	2.87	-10.03	5.89	12.90	0.35

5NH2 -Tz -3x	9.97	-0.53	18.29	2.72	-9.97	2.16	12.69	0.37
5NH2 -Tz -4x	9.82	-0.27	13.70	3.52	-9.82	6.08	13.34	0.28
5NH2 -Tz -2xq	5.47	-0.63	5.30	2.83	-5.47	7.49	8.30	0.35
5NH2 -Tz -3xq	5.46	-0.61	5.47	2.72	-5.46	2.64	8.18	0.37
5NH2 -Tz -4xq	5.30	-0.32	4.24	3.31	-5.30	7.53	8.60	0.30
5-Ph-Tz -2x	9.27	-1.62	20.94	2.05	-9.27	6.43	11.73	0.49
5-Ph-Tz -3x	9.14	-1.73	19.98	2.09	-9.14	4.26	11.23	0.48
5-Ph-Tz -4x	9.29	-1.34	17.67	2.44	-9.29	1.01	11.32	0.41
5-Ph-Tz -2xq	4.60	-1.92	3.97	2.67	-4.60	9.36	8.00	0.38
5-Ph-Tz -3xq	5.38	-1.83	6.06	2.39	-5.38	6.41	7.76	0.42
5-Ph-Tz -4xq	5.49	-1.40	6.00	2.51	-5.49	0.43	7.27	0.40
5NH2 -Tz -2x	10.03	-0.53	17.54	2.87	-10.03	5.89	12.90	0.35
5NH2 -Tz -3x	9.97	-0.53	18.29	2.72	-9.97	2.16	12.69	0.37
5NH2 -Tz -4x	9.82	-0.27	13.70	3.52	-9.82	6.08	13.34	0.28
5NH2 -Tz -2xq	5.47	-0.63	5.30	2.83	-5.47	7.49	8.30	0.35
5NH2 -Tz -3xq	5.46	-0.61	5.47	2.72	-5.46	2.64	8.18	0.37
5NH2 -Tz -4xq	5.30	-0.32	4.24	3.31	-5.30	7.53	8.60	0.30

The relationship between the experimentally determined inhibition efficiency (IE%) [16] and the corresponding theoretical results was evaluated using correlation analysis, as summarized in Table 4. The analysis revealed the strongest correlations for the Ionization potential (I) and Highest Occupied Molecular Orbital Energy values in the Vapor Phases and aqueous phases, with correlation values of 95% and 89%, respectively. These relatively high values demonstrate a strong relationship between the calculated quantum chemical descriptors and the experimentally measured inhibition efficiency. In addition, satisfactory correlations, exceeding 64%, were obtained for the Total Negative Charge values, Electron affinity, Global Softness, Global Hardness, Energy Gap, Ionization Energy and Highest Occupied Molecular Orbital Energy values. The complete correlation results for the investigated parameters are presented in Table 4.

Table (4): The experimental inhibition efficiency (IE%) Relationship between and the calculated quantum chemical parameters.

Association	I	σ	ELUMO	EHOMO	ΔE	TNC	η	ε	χ	ω	μ
Vapor Phase	0.95	0.73	0.29	0.98	0.69	0.66	0.80	0.19	0.19	0.13	0.23
Liquid Phase	0.89	0.80	0.17	0.88	0.71	0.64	0.88	0.34	0.34	0.04	0.29

Density functional theory calculations provide valuable insights into the structural conformation and molecular behavior of these compounds. Specifically, the theory of function Density approach enables a precise analysis of the electrostatic potential distribution [22]. Figure 4 illustrates the analysis of the electrostatic potential surfaces for the non-protonated forms of the compounds in both Vapor Phase and aqueous phases. The maps of the electrostatic potential are essential for identifying the nucleophilic and electrophilic regions of all molecule, they serve as critical tools for evaluating the reactivity of these compounds [23].

Conclusion:

Based on the quantum-chemical descriptors calculated for the tetrazole-based inhibitors (Tz, 5-Ph-Tz, and 5NH2-Tz), the measured inhibition efficiencies are consistently supported. As a general trend from the chemical softness values, molecules with higher softness typically adsorb more readily on the metal surface. In the gas phase as well as in the aqueous phase, chemical softness is highest for 5-phenyl Tetrazole (5-Ph-Tz) and lowest for tetrazole (Tz); this confirms that 5-phenyl Tetrazole (5-Ph-Tz) works best as an inhibitor, while tetrazole (Tz) works least well. The quantum chemical descriptors computed for the tetrazole-based inhibitors (Tz, 5-Ph-Tz and 5NH2-Tz) consistently line up with the inhibition efficiencies observed in experiments.

From the chemical softness values, it appears that molecules with greater softness tend to adsorb more strongly on the metal surface. In both the gas phase and the water phase, 5-phenyl Tetrazole (5-Ph-Tz) shows the highest softness, whereas tetrazole (Tz) shows the lowest, which confirms 5-phenyl Tetrazole (5-Ph-Tz) as the most effective inhibitor and tetrazole (Tz) as the least. This trend is also backed up by the electronegativity values. Dipole moment analysis further reinforces these findings: higher dipole moments are linked to better electron transport and stronger interactions between the inhibitor and the metal. Among the molecules studied, 5-Amino tetrazole (5NH2-Tz) has the highest dipole moment, which suggests a strong ability to adsorb, especially in both the gas phase and the water phase. Looking at how the total negative charge (TNC) is distributed gives more evidence for how well the tetrazole derivatives under study can be adsorbed.

The fairly high electron density on 5-phenyl tetrazole (5-Ph-Tz) and 5-amino tetrazole (5-NH_2-Tz) makes them better at donating electrons to the empty orbitals of the mild steel surface. This leads to stronger interactions at the interface and more stable layers of adsorbed material. As a result, these derivatives are expected to work better as corrosion inhibitors than the parent tetrazole molecule does. This theoretical picture fits well with the inhibition efficiencies found in experiments, which shows a clear link between the calculated electronic properties and the protection that's seen.

Taken together, the quantum chemical results point to 5-phenyl Tetrazole (5-Ph-Tz) as the most effective corrosion inhibitor, with 5-Amino tetrazole (5NH2 -Tz) coming next and tetrazole (Tz) showing the weakest performance throughout. These calculated findings match what has been seen in experiments, which confirms that quantum chemical modeling can predict corrosion inhibition quite reliably.

A correlation analysis was also carried out between experimental inhibition efficiencies and a number of computed parameters. The strongest links were found for EHOMO and ionization energy (I), which had correlation coefficients of 95% and 89% in gas and water phases, respectively. Good correlations, above 64%, also appeared for ΔE, hardness (η), softness (σ) and TNC, which supports the idea that these descriptors are dependable.

References:

1. Saracoglu, M., Elusta, M. I. A., Kaya, S., Kaya, C., & Kandemirli, F. (2018). Quantum chemical studies on the corrosion inhibition of Fe78B13Si9 glassy alloy in Na2SO4 solution of some thiosemicarbazone derivatives. Int. J. Electrochem. Sci., 13, 8241-8259.
2. Kaya, S., Kaya, C., Guo, L., Kandemirli, F., Tüzün, B., Uğurlu, İ., Madkour, L. H., & Saracoglu, M. (2016). Quantum chemical and molecular dynamics simulation studies on the inhibition performances of some thiazole and thiadiazole derivatives against the corrosion of iron. J. Mol. Liq., 219, 497-504.
3. Dennington, R., Keith, T. A., & Millam, J. M. (2016). GaussView, Version 6, Semichem Inc., Shawnee Mission, KS.
4. Frisch, M. J., Trucks, G. W., Schlegel, H. B., Scuseria, G. E., Robb, M. A., Cheeseman, J. R., Scalmani, G., Barone, Cioslowski, J., & Fox, D. J. (2009). Gaussian 09, Revision A.02, Gaussian Inc., Wallingford, CT.
5. Ebenso, E. E., Arslan, T., Kandemirli, F., Love, I., Öğretir, C., Saracoglu, M., & Umoren, S. A. (2010). Theoretical studies of some sulphonamides as corrosion inhibitors for carbon steel in acidic medium. Int. J. Quantum Chem., 110, 2614-2636.
6. Rao, B. V. A., & Kumar, K. C. (2017). 5-(3-Aminophenyl) tetrazole-A new corrosion inhibitor for Cu–Ni (90/10) alloy in seawater and sulphide containing seawater. Arab. J. Chem., 10, 2245-2259.
7. El-Sayed, M. S., Erasmus, R. M., & Comins, J. D. (2008). Inhibition of copper corrosion in acidic chloride pickling solutions by 5-(3-aminophenyl)-tetrazole as a corrosion inhibitor. Corr. Sci., 50, 3439-3445.
8. El-Sayed, M. S., (2011). Effects of 5-(3-aminophenyl)-tetrazole on the inhibition of unalloyed iron corrosion in aerated 3.5% sodium chloride solutions as a corrosion inhibitor. Mater. Chem. Phys., 129, 961-967.

9. Ostrovskii, V. A., Popova, E. A., & Trifonov, R. E. (2017). Chapter One: Developments in tetrazole chemistry (2009-16). Adv. Hetero. Chem., 123, 1-62.
10. Khaled, K. F. (2010). Studies of iron corrosion inhibition using chemical, electrochemical, and computer simulation techniques. Electrochim. Acta, 55, 6523-6532.
11. Kandemirli, F., Saracoglu, M., Amin, M. A., Basaran, M. A., Vurdu, C. D. (2014). The quantum chemical calculations of serine, therionine and glutamine. Int. J. Electrochem. Sci., 9, 3819-3827.
12. Gece, G., & Bilgiç, S. (2009). Quantum chemical study of some cyclic nitrogen compounds as corrosion inhibitors of steel in NaCl media. Corros. Sci., 51, 1876-1878.
13. Musa, A. Y., Kadhum, A. H., Mohamad, A. B., Rohoma, A. B., & Mesmari, H. (2010). Electrochemical and quantum chemical calculations on 4,4-dimethyloxazolidine-2-thione as an inhibitor for mild steel corrosion in hydrochloric acid. J. Mol. Struct., 969, 233-237.
14. Popova, A., Christov, M., & Deligeorgiev, T. (2003). Influence of the molecular structure on the inhibitor properties of benzimidazole derivatives on carbon steel corrosion in 1 M hydrochloric acid. Corrosion, 59, 756-764.
15. Yıldız, R. (2015). An electrochemical and theoretical evaluation of 4,6-diamino-2-pyrimidinethiol as a corrosion inhibitor for mild steel in HCl solutions. Corros. Sci., 90, 544-553.
16. Guan Luo, Y. C., & Han, K. N., (1998). Corrosion Inhibition of a Mild Steel by Aniline and Alkylamines in Acidic Solutions. Corrosion, 54, 721-731.
17. Khaleda, K. F., & Al-Qahtani, M. M. (2009). The inhibitive effect of some tetrazole derivatives towards Al corrosion in acid solution: Chemical, electrochemical and theoretical studies. Mater. Chem. Phys., 113, 150-158.
18. Martinez, S., & Štagljar, I. (2003). Correlation between the molecular structure and the corrosion inhibition efficiency of chestnut tannin in acidic solutions. J. Mol. Struct., 640, 167-174.
19. Obi-Egbedi, N. O., Obot, I. B., & El-Khaiary, M. I. (2011). Quantum chemical investigation and statistical analysis of the relationship between corrosion inhibition efficiency and molecular structure of xanthene and its derivatives on mild steel in sulphuric acid. J. Mol. Struct.,1002, 86-96.
20. Guo, L., Zhu, S., Zhang, S., He, Q., & Li, W. (2014). Theoretical studies of three triazole derivatives as corrosion inhibitors for mild steel in acidic medium. Corros. Sci., 87, 366-375.
21. Hasanov, R., Sadıkoglu, M., & Bilgiç, S. (2007). Electrochemical and quantum chemical studies of some Schiff bases on the corrosion of steel in H2SO4 solution. Appl. Surf. Sci., 253, 3913-3921.
22. Ebenso, E. E. (2003). Synergistic effect of halide ions on the corrosion inhibition of aluminium in H2SO4 using 2-acetylphenothiazine. Mater. Chem. Phys., 79, 58-70. Kaya, S., Kaya, C., & Islam, N. (2016). Reactivity dynamics in atom−field interactions: a quantum fluid density functional study. Comput. Theor. Chem., 1080, 72-78.
23. Cárdenas-Galindo, L. E., & Islas, A. (2015). Synthesis of Novel Bis-1,5-Disubstituted-1H-Tetrazoles by an Efficient Catalyst-Free Ugi-Azide Repetitive Process. Molecules, 20, 1519-1526.
24. Cárdenas-Galindo, L. E., & Islas, A., (2015). Synthesis of Novel bis-1,5-Disubstituted-1H-Tetrazoles by an Efficient Catalyst-Free Ugi-Azide Repetitive Process. Molecules, 20, 1519-1526.